Removal of Ni(II) Ions by Citric Acid-Functionalised *Aloe vera* Leaf Powder – Characterisation, Kinetics, and Isotherm Studies

Waheeba Ahmed Al-Amrani[1], Rohaizan Abdullah[2],
Megat Ahmad Kamal Megat Hanafiah[2*], Faiz Bukhari Mohd Suah[3]

[1] Department of Chemistry, College of Science, Ibb University, Ibb, Yemen

[2] Faculty of Applied Sciences, Universiti Teknologi MARA Pahang, 26400, Jengka, Pahang, Malaysia

[3] School of Chemical Sciences, Universiti Sains Malaysia, 11800, Minden, Pulau Pinang, Malaysia

* Corresponding author's e-mail: makmh@uitm.edu.my

ABSTRACT

Aloe vera leaves (AVL), a by-product of agricultural waste, have been applied as a biosorbent for reducing Ni(II) ions in aqueous solutions. The biosorption capability of AVL powder was enhanced through chemical treatment with 0.10 M citric acid solution. Fourier-transform infrared (FTIR) spectrophotometer, scanning electron microscope coupled with energy dispersive X-ray (SEM-EDX), pH of point-zero-charge (pH_{PZC}), and pH_{slurry} analyses were used to study the surface, and chemical properties of citric acid-treated *Aloe vera* leaf powder (CAAVLP). The setting for experiments such as pH solution, CAAVLP dose, initial concentration, and biosorption time was investigated. Maximum Ni(II) ion biosorption capability was determined to be 48.65 mg/g based on the Langmuir model at pH 6, a CAAVLP dose of 0.02 g, initial Ni(II) concentrations of 5 to 50 mg/L and biosorption time of 120 min. The data for the isotherm and kinetics were well matched with the Freundlich and pseudo-second-order models, respectively, with high regression correlation (R^2) and low chi-square (χ^2) values. The presence of more -COOH groups after treating AVL with citric acid resulted in more Ni(II) ions being able to be removed.

Keywords: *Aloe vera*; biosorption; isotherm; nickel; wastewater.

INTRODUCTION

Rapid industrialisation has resulted in releasing harmful chemicals into the environment above permitted levels, which has contaminated the land, water, and air. Over time, these contaminants become more concentrated in ground and surface water due to anthropogenic activities. Because of the long-term and short-term impacts that heavy metals have on people and other species, they have been classified as extremely harmful contaminants. Chemical decomposition is not an option for heavy metals and can build up in the body, harming all life systems [Gautam et al., 2015; Pujari and Kapoor, 2021]. Removing heavy metals from effluents is essential since they are primarily responsible for heavy metal pollution in the textile, electroplating, painting, dyeing, and chemical industries.

One of the top 25 elements by abundance in the Earth's crust is nickel (Ni), which is discharged into the environment due to nickel mining or a number of industrial processes, including those used in plastic and rubber industries, electroplating, and nickel-cadmium battery manufacturing. Nickel's widespread presence in the workplace and applications have both been shown to have negative effects on human health. Nickel is non-biodegradable and has carcinogenic, teratogenic, and mutagenic properties. Long-term nickel exposure can lead to cancer, lung fibrosis, and dermatitis (eczema) [Das et al., 2019]. The World Health Organization (WHO) recommends keeping Ni(II) ion concentrations in industrial wastewater below 2.0 mg/L [Gupta and Kumar, 2019]. As a result, getting rid of Ni(II) ions from industrialised wastewater before releasing it into the environment is a very important issue.

Ni(II) ions can be removed from industrial effluents through a number of different physicochemical processes, all of which have varying degrees of success, such as electrocoagulation [Akbal and Camc, 2011], filtration [Vengatajalapathi et al., 2022], biosorption [Qu et al., 2019], ion exchange [Strauss et al., 2021], aerobic and anaerobic treatment [An et al., 2021, Costa et al., 2022], solvent extraction [Zhang et al., 2021], and electrolysis [Wang et al., 2021]. Due to its many benefits over alternative techniques, such as its low cost, straightforward design, simplicity of use, and adaptability, the biosorption method has long attracted the attention of scientists. It is believed that biosorption technology has great potential for removing hazardous pollutants [Hu and Xu, 2020]. Biosorbents that are commonly used, for instance, activated carbon, metal nanoparticles, and graphene, are costly and have low recyclability [Ogunlalu et al., 2021]. As a result, there is a need to search for new biosorbents that are widely available, renewable and cheap. Agro-industrial waste products can meet these criteria because of their low cost and high abundance [Rajczykowski et al., 2018, Hoang et al., 2020, Chand et al., 2021]. Nevertheless, due to concerns like low metal removal efficiency, low surface area, and low biosorption dynamic sites, they need to be modified with other chemicals before they can be used [Ogunlalu et al., 2021]. Currently, potentially modified biosorbents including plant biomass that is non-living [Tiwari et al., 2022], leaves [Gupta and Kumar, 2019], bark [Reddy et al., 2011, Qu et al., 2019], and peel wastes [Tejada-Tovar et al., 2021] have been used to treat aqueous solutions containing Ni(II) ions.

Aloe vera is regarded as one of the most important medicinal plants with an extensive range of applications due to the abundance of bioactive compounds in its leaves. Since ancient times, it has been linked to various health benefits, including the ability to treat wounds, fight free radicals, prevent cancer, modulate the immune system, and even act as a laxative. The use of *Aloe vera* extends far beyond the pharmaceutical and medical fields. As of late, *Aloe vera* and its wares have become increasingly popular for environmental applications [Giannakoudakis et al., 2018]. About 65% of the fresh *Aloe vera* leaves are left as waste after they have been processed. Aloin has hydroxyl groups, and its derivatives are the major components of *Aloe vera* leaf wastes. The use of aloin and its derivatives has been prohibited in the United States since 2002. Because of this, these industries consider this residue to be waste, and it can be used as a biosorbent [Gupta and Kumar, 2019]. The waste can be used as is or after being modified. Both acid and alkaline chemicals can be used to modify raw waste biomass. For instance, Gupta et al. (2019) used various acid and alkaline chemicals to treat *Aloe vera* waste and established that *Aloe vera* leaf waste had a low biosorption ability for Cd(II) ions and Ni(II) ions. In another study, Gupta et al. (2019) used a pressure cooker to steam-heat *Aloe vera* waste for 20 minutes at a high pressure of 15 psi, and the Ni(II) biosorption capacity was only 10 mg/g. However, when the steam-heated *Aloe vera* was mixed with 0.10 mol/L aqueous solution of Na_2CO_3, the biosorption capacity increased to 28.98 mg/g [Gupta et al., 2019].

For metal ions, citric acid, a common organic acid, has a strong chelating ability, which facilitates biosorption. Few works on the biosorption of Ni(II) ions onto citric-modified biosorbents, such as sugarcane bagasse [Hoang et al., 2020] and water hyacinth [Qu et al., 2019], have been conducted. To our knowledge, there has been no investigation into the efficacy of treating Aloe vera with citric acid to get rid of Ni(II) ions from wastewater. In light of the preceding observations, this research intends to examine the effectiveness of biosorption of Ni(II) ions from a synthetic watery medium by citric acid-modified Aloe vera leaf powder as a biosorbent. The effects of pH solution, biosorbent dose, initial Ni(II) ions concentration, and biosorption time on Ni(II) ions biosorption were investigated. The biosorption equilibria and kinetics parameters were also investigated. Furthermore, this biosorbent was characterised before and after treatment with citric acid throughout aspects of FTIR, SEM-EDX, pH_{PZC} and pH_{slurry}.

MATERIALS AND METHODS

Preparation of biosorbent

The *Aloe vera* (*Aloe barbadensis* Miller) leaves were obtained from a garden in Jengka, Malaysia. The gel and yellow saps were removed, leaving the green leaves used in the biosorption experiments. Numerous rinses with distilled water were used to thoroughly clean the leaves before being dried in an electric oven at 110 °C for

24 h until they reached a constant weight. Before being labelled as *Aloe vera* leaf powder (AVLP), the leaves were crushed and sieved to get the particles down to 180 mesh. Then, 25.0 g of AVLP was treated with 500 mL of 0.10 M citric acid for 1 h at room temperature, thoroughly mixed and agitated, and finally washed with distilled water to remove the excess acid and labelled as CAAVLP. To preserve it for future study, the CAAVLP was placed in an airtight container.

Characterisation of biosorbent

FTIR (PerkinElmer, Spectrum 100, USA) and SEM (Carl Zeiss SMT, Germany) coupled with energy dispersive X-ray (EDX, Oxford Instrument, UK) instruments were applied to examine the functional groups and surface possessions of the AVLP and CAAVLP, as well as the Ni(II) ions-loaded CAAVLP biosorbent. Mixing 0.50 g of CAAVLP with 50 mL of distilled water for 24 h at 29 °C allowed for the calculation of the slurry's pH. After filtration using No. 42 Whatman filter paper, the final pH was determined using a pH meter. The pH_{PZC} of CAAVLP was conducted by preparing a series of 50 mL (0.01 M) NaCl solutions with initial pH (pH_i) values ranging from 2 to 10 in 50 mL conical flasks. After adding 0.50 g of CAAVLP to the NaCl solutions, the mixture was stirred for 24 h using a magnetic stirrer. The solution's final pH (pH_f) was determined after filtration. The curve that intersected the pH_i axis in the pH_i–pH_f versus pH_i plot represented the value of pH_{PZC} of CAAVLP.

Preparation of adsorbate

Water-based solutions containing 97% pure Ni(II) ions in the form of $Ni(NO_3)_2.6H_2O$ were utilised in biosorption experiments. By dissolving 4.995 g of $Ni(NO_3)_2.6H_2O$ in 1 L of purified water, 1000 mg/L standard solution Ni(II) ions was produced. Unless otherwise specified, all chemicals used in this study were of analytical reagent grade.

Batch biosorption studies

Batch biosorption tests were done in conical flasks with lids, stirred at 200 rpm with a magnetic stirrer for 120 min using 50 mL of Ni(II) ions from the standard solution. The pH ranged from 2 to 6, and the CAAVLP amount ranged from 0.02 to 0.10 g were selected to investigate the effects of pH and biosorbent dosage on the ability of CAAVLP to biosorb 20 mg/L of Ni(II) ions, respectively. The working solutions' pH was initially adjusted with 0.10 M HCl or NaOH solutions using a pH meter (EUTECH Instruments, USA). As Ni(II) ions precipitation could occur at a pH above 6 [Gupta and Kumar, 2019], higher pH values were not chosen for the current study. The biosorption kinetics of CAAVLP at different biosorption times ranging from 5 to 120 min at pH 6 were studied using three Ni(II) concentrations of 5, 10, and 20 mg/L. The Ni(II) ion concentrations selected were 5 to 50 mg/L in the isotherm study. After reaching equilibrium, the concentration was determined using an Atomic Absorption Spectrometer (PerkinElmer, PinAAcle 900T model, USA). All of the biosorption experiments were done twice, and the results are presented as the average. The following equation was used to find out how effectively CAAVLP could biosorb Ni(II) ions:

$$q_e = \frac{(C_i - C_e) \times V}{W} \qquad (1)$$

where: q_e (mg/g) is the quantity of Ni(II) ions biosorbed at equilibrium state;
C_i (mg/L) is the initial concentration of Ni(II) ions;
C_e (mg/L) is the equilibrium concentration of Ni(II) ions;
W (g) is the quantity of CAAVLP;
V (L) is the volume of Ni(II) ions solution.

RESULTS AND DISCUSSION

Characterisation of biosorbent

Figure 1(a, b) depicts *Aloe vera* before and after treatment with citric acid. It can be seen that AVLP (before citric acid treatment) is darker than CAAVLP (after treatment with citric acid). The FTIR spectra of AVLP, CAAVLP, and Ni-overloaded CAAVLP were measured in the 4000 to 600 cm^{-1} wavenumber range and are depicted in Figure 2 and Table 1. The FTIR spectrum of AVLP showed numerous distinct groups to a certain extent of 3500 cm^{-1} to 3200 cm^{-1} indicating the existence of stretching O-H groups. The biosorption peaks in 2917 to 2851 cm^{-1} as a result of vibration stretching of C-H groups. The biosorption peak at 1731 cm^{-1} represents –C=O stretching

Table 1. FTIR Characteristics of CAAVLP before and after Ni(II) ions uptake

Wavenumber range (cm⁻¹)	Before uptake	After uptake	Difference in shift	Assignment
3500–2500	3333	3334	+1	-OH. -NH and COOH groups
2950–2800	2920	2919	-1	-C-H stretching
1740–1680	1731	1730	-1	-C=O carbonyl group
1670–1500	1623	1620	-3	-COO⁻ carboxylic and C=C aromatic groups
1150–1020	1012	1019	+7	-C-O-C stretching bond

carbonyl groups. Functional groups around 1600 cm⁻¹ are indicative of carboxylic acid groups. The biosorption peak at 1418 cm⁻¹ signifies aromatic ring C-H bending. The strong peak at 1020 cm⁻¹ indicates -C-O-C- while the biosorption peak at 768 cm⁻¹ aromatic ring C-H bending (getting of the plane) [Gupta et al., 2019, Ezeonuegbu et al., 2021]. The same characteristic bands were found in the CCAVLP spectrum. Thus, hydroxyl, carboxylic, aldehydes, phenol, ketones, ester, and aromatic rings are all present in both AVLP and CAAVLP (i.e. derived from polysaccharides such

Figure 1. *Aloe vera* leaf powder (a) AVL powder (before treatment with citric acid) and (b) CAAVLP powder (after treatment with citric acid)
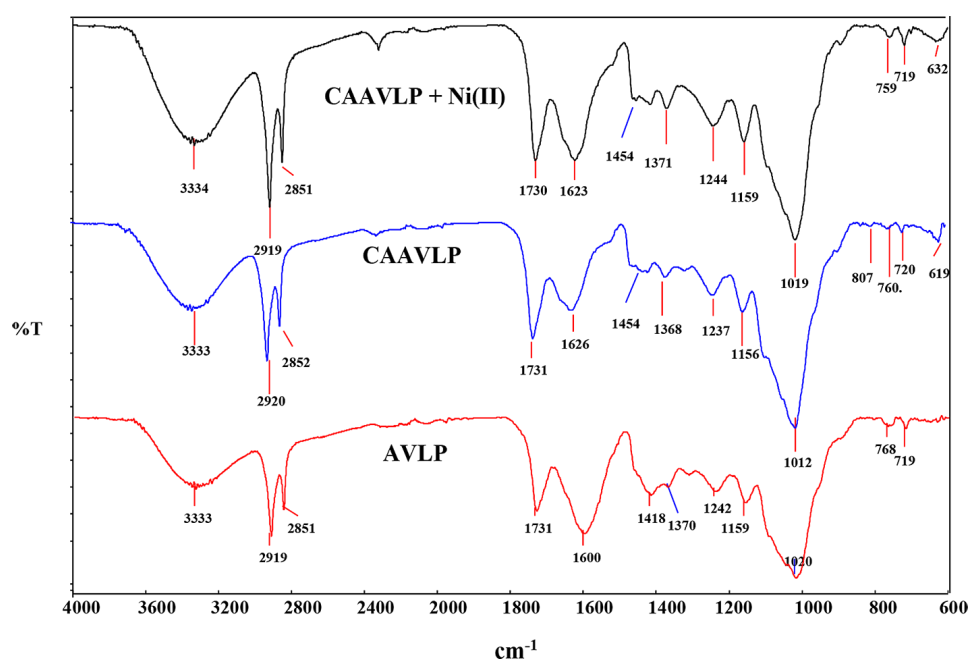
Figure 2. FTIR spectra of the AVLP and CAAVLP (before and after Ni(II) ions biosorption)

as glucans, lignin, anthraquinones and uric acid) [Gupta et al., 2019, Ezeonuegbu et al., 2021]. After loading the CAAVLP with Ni(II) ions, the biosorbent's peak intensities either increased or shifted slightly as shown in Table 1. These observations highlighted that carboxyl, hydroxyl, and aromatic groups were all involved in Ni(II) biosorption, which could occur via ionic attraction and weak electrostatic attraction in addition to complexation interactions [Gupta et al., 2019, Ezeonuegbu et al., 2021].

Figure 3a and 3b shows SEM and EDX images of CAALVP and Ni(II)-exhausted CAALVP, respectively. Because of the presence of longitudinal tissue, the CAAVLP biosorbent has a porous and irregular surface, as shown in Fig. 3A1. It also has essential elements such as Ca^{2+}, C, O, and Au on its surface, as shown in Figs. 3 (A2, A3). After CAAVLP was loaded with Ni(II) ions, the biomatrix sorbent's surface's layers shrank and new shiny bulky layers appeared (Fig. 3B1), which were not present in the raw CAAVLP biosorbent
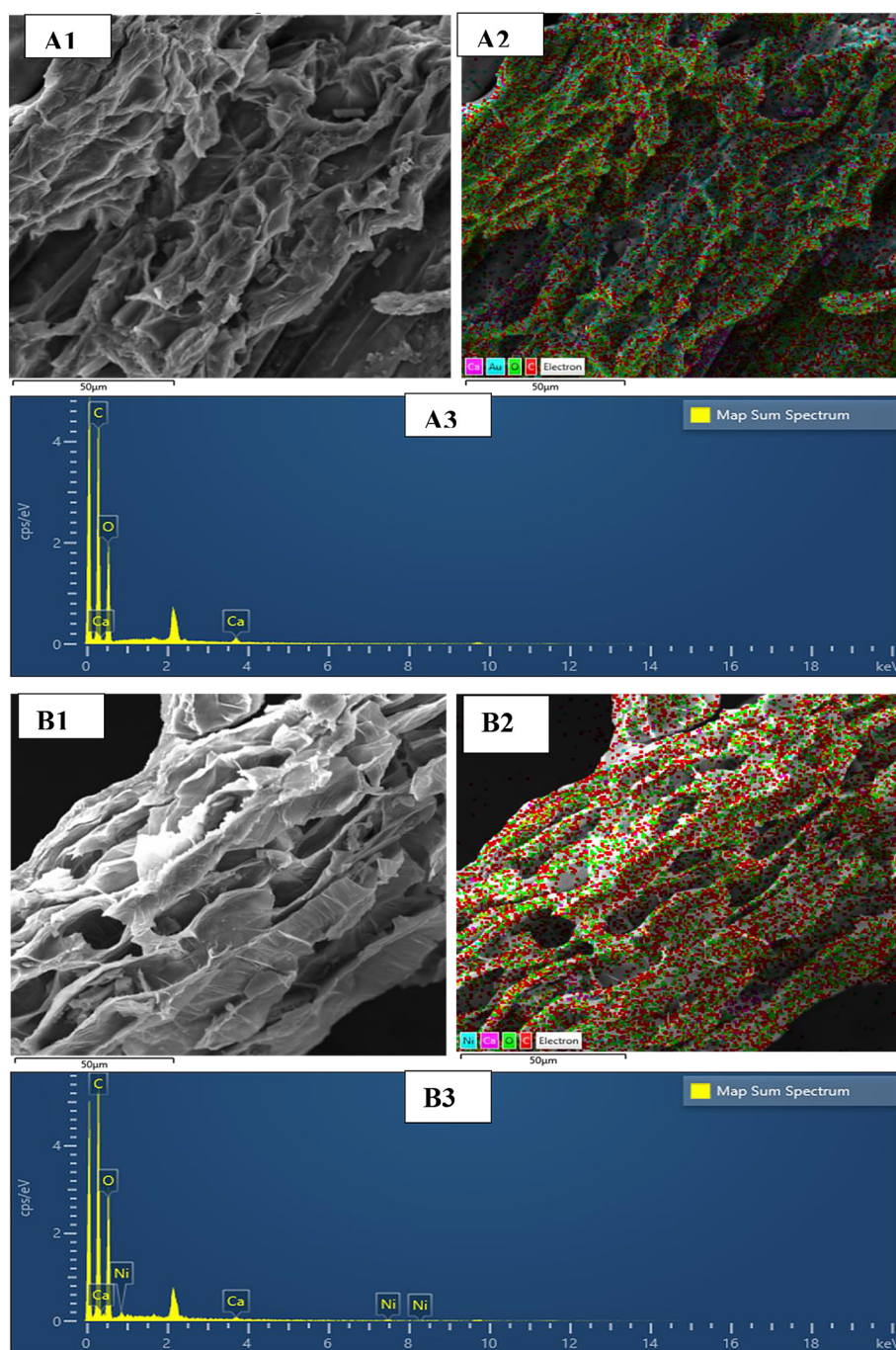
Figure 3. SEM images (1000x magnification) and EDX images of CAAVLP
(A 1-3) and Ni(II)-loaded CCAVLP (B 1-3), respectively

(Fig. 3A1). This morphological shift can be attributed to the robust cross-linking of Ni(II) ions. The SEM-EDX images, as presented in Figure 3 (B2 and B3), also confirmed the presence of Ni(II) on CAAVLP. The pH_{slurry} of the CAAVLP biosorbent was 4.56. The carboxylic acid groups were responsible for the acidic nature of CAAV-LP, as established by the FTIR spectrum. Figure 4 depicts the pH_{PZC} plot with a value of 4.0. At pH greater than pH_{PZC}, the biosorption of Ni(II) ions would be aided by the increased negative charge on the CCAVLP surface.
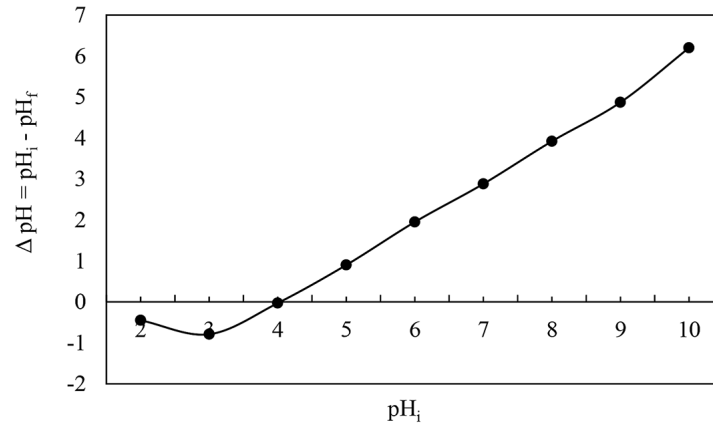
Figure 4. pH_{PZC} plot of CAAVLP (CAAVLP weight – 0.5 g, working volume – 50 mL, [NaCl] – 0.01 M, contact time – 24 h)
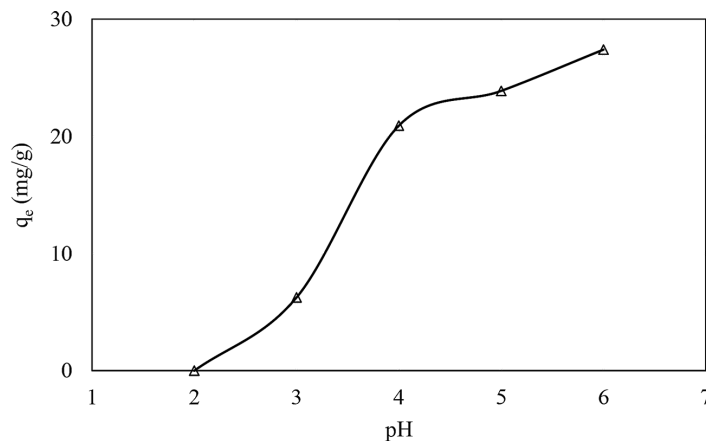
Figure 5. Effect of pH on Ni(II) biosorption (CAAVLP weight – 0.02 g, pH – 2–6, working volume – 50 mL, [Ni^{2+}] – 20 mg/L, contact time – 120 min)
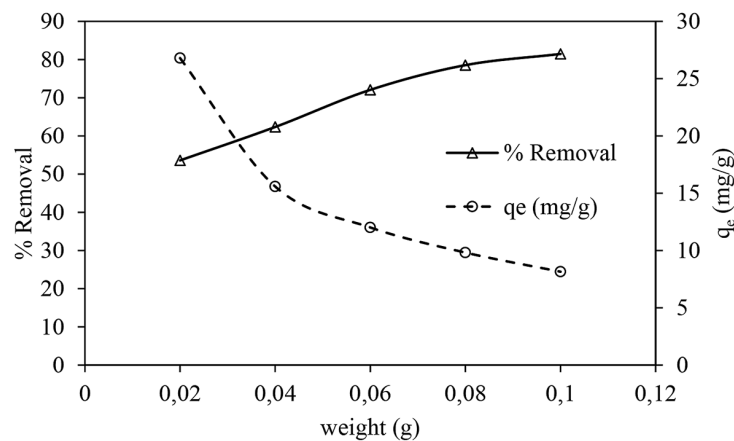
Figure 6. Effect of CAAVLP dosage on Ni(II) biosorption (CAAVLP weight – 0.02–0.1 g, pH 6, working volume – 50 mL, [Ni^{2+}] – 20 mg/L, contact time – 120 min)

EFFECT OF OPERATIONAL PARAMETERS

Effect of pH

The pH is the most influential parameter on metal ion solubility, counter ion concentration on biosorbent functional groups, and adsorbate ionization during a chemical reaction. Figure 5 depicts the effect of pH solution on the biosorption of Ni(II) ions onto CAAVLP. Ni(II) biosorption increases with increasing solution pH, with maximum removal occurring at pH6. Nickel uptake was inhibited at low pH levels, possibly owing to biosorption site competition between hydrogen and nickel ions [Beidokhti et al., 2019].

Effect of biosorbent dosage

Figure 6 depicts the influence of biosorbent dose on the CAAVLP-mediated biosorption of Ni(II) ions. It can be seen that once the CAAVLP amount was arrised up from 0.02 g to 0.1 g, the biosorption efficiency improved gradually from 53.60% to 81.48%. It could be ascribed to the presence of extra biosorption sites on the bio-surface [Ezeonuegbu et al., 2021]. With increasing CAAVLP dosage, the amount of Ni(II) ions biosorbed by the CAAVLP decreased. It could be attributed to biosorption site overlapping or aggregation at increased biosorbent dosages, the exposed surface area for adsorbate biosorption decreased [Ezeonuegbu et al., 2021]. Thus, the following kinetics and isotherm experiments were conducted using 0.02 g of CAAVLP.

Biosorption kinetic studies

Figure 7 depicts the time-dependent changes in the quantity of Ni(II) ions biosorbed on CAAVLP at different initial concentrations of Ni(II) ions, namely 5, 10, and 20 mg/L. Early on in the biosorption process (between 0 and 5 minutes), a substantial change in the quantity of Ni(II) ions biosorbed was noticed, indicating that the biosorbent had a high availability of free binding sites. Following that, the slow biosorption process was observed between 5 and 20 minutes due to the intense competition between Ni(II) ions regarding the rest of the biosorption sites that are functional. Finally, the steadiness biosorption progression was completed in 20 to 120 minutes, there was just slight shift in the total quantity of Ni(II) ions biosorbed after the biosorption sites became fully saturated. Similar outcomes were observed when Ni(II) was biosorbed using pistachio hull waste [Beidokhti et al., 2019], *Lycopersicum esculentum* (tomato) [Yuvaraja Gutha et al., 2014] and *Moringa oleifera* bark [Reddy et al., 2011]. In addition, the quantity of Ni(II) ions biosorbed increased with the increase of the initial Ni(II) ions concentration. This may be due to the fact that higher Ni(II) ion concentrations have a stronger driving force, allowing them to overcome the biosorbent-liquid mass transfer resistance [Hanafiah et al., 2022].

To investigate further the biosorption rate of Ni(II) ions, the biosorption data in Figure 7 were analysed using non-linear kinetics models. Pseudo-first order (PFO) [Lagergren, 1898] and pseudo-second-order (PSO) [Ho and McKay, 1999] in nonlinear systems were given by Eqs.
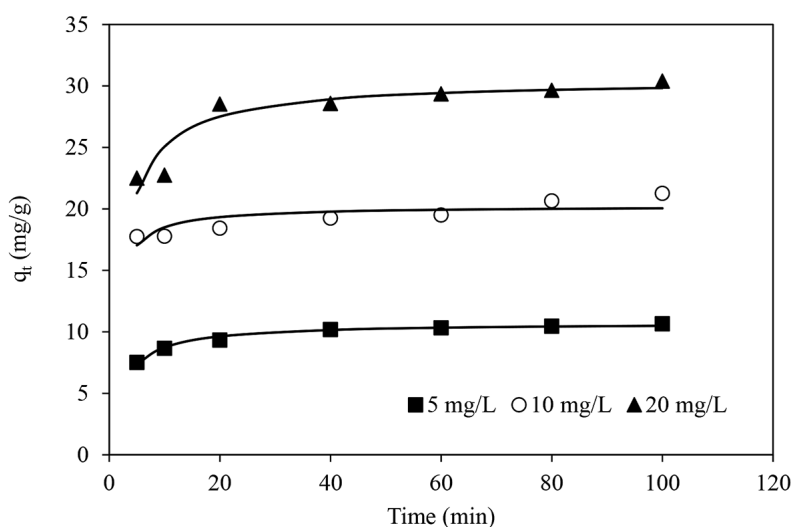
Figure 7. Effect of contact time using three different initial concentrations on Ni(II) biosorption on CCAVLP

Table 2. Pseudo-first-order and pseudo-second-order kinetics parameters calculated for Ni(II) ions biosorption on CAAVLP biosorbent

Ni(II) (mg/L)		5	10	20
Pseudo-first-order	$q_{e, exp}$ (mg/g)	10.66	21.27	30.40
	q_e	10.17	19.58	28.99
	k_1	0.24	0.44	0.24
	R^2	0.82	0.29	0.69
	χ^2	0.15	0.41	0.84
Pseudo-second-order	$q_{e, exp}$ (mg/g)	10.66	21.27	30.40
	q_e	10.73	20.24	30.48
	k_2	0.04	0.05	0.02
	R^2	0.98	0.62	0.87
	χ^2	0.02	0.22	0.34

2 and 3, respectively. The determiner coefficient (R^2) and the chi-square test (χ^2), Eq. 4, were applied to ascertain which model was most effectively fitted to the experimental data [Ezeonuegbu et al., 2021].

$$q_t = q_e(1 - e^{k_1 t}) \qquad (2)$$

$$q_t = \frac{q_e^2 k_2 t}{(1 + k_2 q_e t)} \qquad (3)$$

$$\chi^2 = \sum \frac{(q_e^{exp} - q_e^{cal})^2}{q_e^{cal}} \qquad (4)$$

where: q_e and q_t (mg/g) refer to the quantity of Ni(II) ions at steadiness state at time, t, respectively.
The k_1 and k_2 characterise the total rate constants of PFO (1/min) and PSO (g.mg/min) models.
The q_e^{exp} and q_e^{cal} (mg/g) symbolise the quantity of Ni(II) ions biosorbed at steadiness state dogged as of the experimental and calculated one from the model, respectively.

The kinetic constants calculated using the nonlinear models are shown in Table 2, as well as the regression correlation coefficient (R^2) and chi-square (χ^2) values. As can be seen, the PSO model fit the experimental data well. The calculated values of q_e for the PFO model did not match the experimental values, while R^2 was lower and higher χ^2 than for the PSO model. This demonstrated that the PFO model was ineffective in explaining the kinetics of the biosorption process. Researchers who used the same methodology reached the same conclusions [Reddy et al., 2011, Ezeonuegbu et al., 2021].

Biosorption isotherm studies

In this study, the experimental data were modeled using two isotherms, namely [Langmuir, 1918] through Eq. 5 and [Freundlich, 1926] by Eq. 6 isotherms.

$$q_e = \frac{Q_{max} K_L C_e}{1 + K_L C_e} \qquad (5)$$

$$q_e = K_F C_e^{1/n} \qquad (6)$$

where: Q_{max} (mg/g) is the theoretical biosorption capability;
K_L (L/mg) is the Langmuir isotherm parameter which is proportional to the strength of the interaction between the biosorbent and the adsorbate;
K_F and n are the Freundlich parameters concerning the biosorption capability and intensity, respectively.

Table 3 displays the Langmuir and Freundlich parameters derived for each model using nonlinear regression. Figure 8 demonstrates that the Freundlich model is a well fit for the investigational

Table 3. Isotherm parameters of Ni(II) ions biosorption deduced from the nonlinear Langmuir and Freundlich models

Isotherm model	Parameter	Value
Langmuir	Q_{max}, (mg/g)	48.65
	K_L, (L/mg)	0.10
	R^2	0.94
	χ^2	6.55
Freundlich	K_F, (L/mg)	8.79
	n	0.43
	R^2	0.99
	χ^2	0.45

Table 4. Comparison of CAAVL biosorption capacity for Ni(II) ions by different biosorbents

Biosorbent	Adsorption capacity (mg/g)	pH	Temp. (K)	Equilibrium time (min)	Reference
Na_2CO_3-modified steam-heated *Aloe vera* leaf powder	28.99	7	303	90	Gupta et al. (2019)
Steam-heated *Aloe vera* leaf powder	10.00	7	303	180	Gupta and Kumar (2019)
Lemon peel	7.4	6	298	120	Tejada-Tovar et al. (2021)
Cassava peel	6.4	6	298	120	Tejada-Tovar et al. (2021)
CAAVLP	48.65	6	302	20	This study
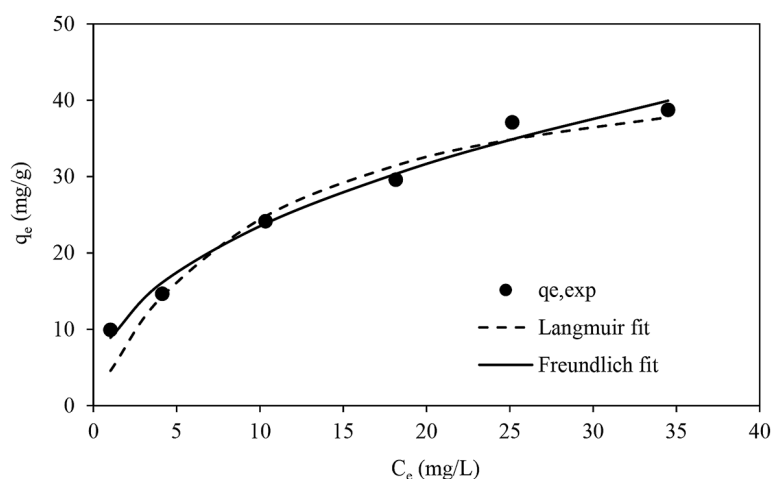
Figure 8. Langmuir and Freundlich isotherm plots of Ni(II) ions biosorption process

data of Ni(II) ion biosorption on CAAVLP than the Langmuir model. Additionally higher R^2 and lower χ^2 values confirm that Freundlich model accurately represents the experimental data as shown in Table 3. The CAAVLP bio-surface sorbent's active sites are not uniformly distributed, suggesting instead the formation of multilayers with varying activation energies that extend from the surface into the pores. Similar findings were reported for a biosorption process that is very similar to it [Ezeonuegbu et al., 2021]. The Langmuir model's Q_{max} is closer to the q_{exp} value, and the value of *n* was less than 1, showing that the biosorption of Ni(II) ions was satisfactory. The Langmuir model was used to figure out that the biosorption capacity of CAAVLP was 48.65 mg/g, which was higher than other studies that used *Aloe vera* as a biosorbent for Ni(II) biosorption, as depicted in Table 4. As a biosorbent, CAAVLP shows promise for cleaning up wastewater with Ni(II) ions.

CONCLUSIONS

The citric acid-treated *Aloe vera* biomass (CAAVLP) had effectively reduced Ni(II) ion concentrations in aqueous solutions. The investigation confirmed that the addition of 0.10 M citric acid to *Aloe vera* leaf powder increased its biosorption capacity for Ni(II) ions relative to other previously reported modifications. Groups of hydroxyl, amino, aromatics, ether and carboxyl were possibly involved in the Ni(II) ions binding route, as revealed by the FTIR spectra. The batch research parameters, including pH solution, CAAVLP dosage, initial Ni(II) concentration, and biosorption time, had a substantial influence on the Ni(II) ions biosorption process. The biosorption process was found to be directed by the PSO kinetic model and the Freundlich model. The maximum biosorption capacity for CAAVLP towards Ni(II) ions was 48.65 mg/g at pH 6.0. The results indicate that CAAVLP is a promising biosorbent for Ni(II) ions removal.

REFERENCES

1. Akbal, F., Camc, S. 2011. Copper, chromium and nickel removal from metal plating wastewater by electrocoagulation. Desalination, 269, 214–222.
2. An, Q., Deng, S., Liu, M., Li, Z., Wu, D., Wang, T., Chen, X. 2021. Study on the aerobic remediation

of Ni (II) by *Pseudomonas hibiscicola* strain L1 interaction with nitrate. Journal of Environmental Management, 299, 113641.

3. Beidokhti, M.Z., Naeeni, S.T.O., AbdiGhahroudi, M.S. 2019. Biosorption of nickel (II) from aqueous solutions onto pistachio hull waste as a low-cost biosorbent. Civil Engineering Journal, 5, 447–457.

4. Chand, A., Chand, P., Khatri, G.G., Paudel, D.R. 2021. Enhanced removal efficiency of arsenic and copper from aqueous solution using activated *Acorus calamus* based adsorbent. Chemical and Biochemical Engineering Quarterly, 35, 279–293.

5. Costa, J.M., da Costa, J.G.d.R., de Almeida Neto, A.F. 2022. Techniques of nickel (II) removal from electroplating industry wastewater: Overview and trends. Journal of Water Process Engineering, 46, 102593.

6. Das, K.K., Reddy, R.C., Bagoji, I.B., Das, S., Bagali, S., Mullur, L., Khodnapur, J.P., Biradar, M.S. 2019. Primary concept of nickel toxicity – an overview. Journal of Basic and Clinical Physiology and Pharmacology, 30, 141–152.

7. Ezeonuegbu, B.A., Machido, D.A., Whong, C.M.Z., Japhet, W.S., Alexiou, A., Elazab, S.T., Qusty, N., Yaro, C.A., Batiha, G.E.-S. 2021. Agricultural waste of sugarcane bagasse as efficient adsorbent for lead and nickel removal from untreated wastewater: Biosorption, equilibrium isotherms, kinetics and desorption studies. Biotechnology Reports, 30, e00614.

8. Freundlich, H. 1926. Colloid and Capillary Chemistry. Methuen, London.

9. Gautam, R.K., Sharma, S.K., Mahiya, S., Chattopadhyaya, M.C. 2015. Chapter 1: Contamination of Heavy Metals in Aquatic Media: Transport, Toxicity and Technologies for Remediation. Heavy Metals In Water: Presence, Removal and Safety. The Royal Society of Chemistry.

10. Giannakoudakis, D.A., Hosseini-Bandegharae, A., Tsafrakidou, P., Triantafyllidis, K.S., Kornaros, M., Anastopoulos, I. 2018. *Aloe vera* waste biomass-based adsorbents for the removal of aquatic pollutants: A review. Journal of Environmental Management, 227, 354–364.

11. Gupta, S., Kumar, A. 2019. Removal of Nickel (II) from aqueous solution by biosorption on *A. barbadensis* Miller waste leaves powder. Applied Water Science, 9, 96.

12. Gupta, S., Sharma, S.K., Kumar, A. 2019. Biosorption of Ni(II) ions from aqueous solution using modified *Aloe barbadensis* Miller leaf powder. Water Science and Engineering, 12, 27–36.

13. Hanafiah, M.A.K.M., Abu Bakar, N.A., Al-Amrani, W.A., Ibrahim, S., Nik Malek, N.A.N., Jawad, A.H. 2022. Preparation, characterization and application of sulphuric acid-treated soursop (*Annona muricata*

L.) seeds powder in the adsorption of Cu(II) ions. Nature Environment and Pollution Technology, 21, 217–223.

14. Ho, Y.S., McKay, G. 1999. Pseudo-second order model for sorption processes. Process Biochemistry, 34, 451–465.

15. Hoang, M.T., Pham, T.D., Pham, T.T., Nguyen, M.K., Nu, D.T.T., Nguyen, T.H., Bartling, S., Van der Bruggen, B. 2020. Esterification of sugarcane bagasse by citric acid for Pb^{2+} adsorption: effect of different chemical pretreatment methods. Environmental Science and Pollution Research.

16. Hu, H., Xu, K. 2020. Chapter 8 – Physicochemical technologies for HRPs and risk control. In: Ren, H., Zhang, X. (Eds.) High-Risk Pollutants in Wastewater. Elsevier.

17. Lagergren, S., Svenska, B.K. 1898. Zurtheorie der sogenannten adsorption geloesterstoffe. Veternskapsakad Handlingar, 24, 1–9.

18. Langmuir, I. 1918. The adsorption of gases on plane surfaces of glass, mica and platinum. Journal of American Chemical Society, 40, 1361e1403.

19. Ogunlalu, O., Oyekunle, I.P., Iwuozor, K.O., Daniel Aderibigbe, A., Emenike, E.C. 2021. Trends in the mitigation of heavy metal ions from aqueous solutions using unmodified and chemically-modified agricultural waste adsorbents. Current Research in Green and Sustainable Chemistry, 4, 100188.

20. Pujari, M., Kapoor, D. 2021. Chapter 1: Heavy metals in the ecosystem: Sources and their effects. In: Kumar, V., Sharma, A.,Cerdà, A. (eds.) Heavy Metals in the Environment. Elsevier.

21. Qu, W., He, D., Guo, Y., Tang, Y., Shang, J., Zhou, L., Zhu, R., Song, R.-J. 2019. Modified water hyacinth functionalized with citric acid as an effective and inexpensive adsorbent for heavy metal ions removal. Indusrial Engineering Chemistry Research, 1–33.

22. Rajczykowski, K., Sałasińska, O., Loska, K. 2018. Zinc removal from the aqueous solutions by the chemically modified biosorbents. Water, Air& Soil Pollution, 229.

23. Reddy, D.H.K., Ramana, D., Seshaiah, K., Reddy, A. 2011. Biosorption of Ni (II) from aqueous phase by Moringa oleifera bark, a low cost biosorbent. Desalination, 268, 150–157.

24. Strauss, M., Diaz, L., McNally, J., Klaehn, J., Lister, T. 2021. Separation of cobalt, nickel, and manganese in leach solutions of waste lithium-ion batteries using Dowex M4195 ion exchange resin. Hydrometallurgy, 206, 105757.

25. Tejada-Tovar, C., Acevedo, D., Villabona-Ortíz, A., Pájaro-Gómez, N., Otero, M. 2021. Comparative study using raw and treated cassava and lemon residues in the removal if Nickel (II). Agrociencia.

26. Tiwari, S., Aachhera, S., Garg, H., Rojra, M., Nagar, N., Gahan, C.S. 2022. Comparative biosorption kinetics study of Ni and Zn metal ions from the aqueous phase in sulfate medium by the wooden biomass of *Dalbergia sissoo*. Environmental Quality Management, 31, 63–73.

27. Vengatajalapathi, N., Ayyappan, S., Rajasekar, V. 2022. Eco-friendly filtration of Nickel from the sludge during electrochemical machining of Monel 400 alloys. Global NEST Journal, 24, 203–211.

28. Wang, C., Li, T., Yu, G., Deng, S. 2021. Removal of low concentrations of nickel ions in electroplating wastewater by combination of electrodialysis and electrodeposition. Chemosphere, 263, 128208.

29. Yuvaraja Gutha, Venkata Subbaiah Munagapati, Mu. Naushad, Abburi, K. 2014. Removal of Ni(II) from aqueous solution by *Lycopersicum esculentum* (Tomato) leaf powder as a low-cost biosorbent. Desalination and Water Treatment.

30. Zhang, L., Ji, L., Li, L., Shi, D., Xu, T., Peng, X., Song, X. 2021. Recovery of Co, Ni, and Li from solutions by solvent extraction with β-diketone system. Hydrometallurgy, 204, 105718.